6th International Conference on Advances in Experimental Structural Engineering
11th International Workshop on Advanced Smart Materials and Smart Structures Technology
August 1-2, 2015, University of Illinois, Urbana-Champaign, United States

Fragility Analysis of Structures Incorporating Control Systems

A.K. Wilbee[1], F. Pena[2], J. Condori[2], Z. Sun[3], S.J. Dyke[4]

1 *Undergraduate Research Asst., Lyles School of Civil Engineering, Purdue University, West Lafayette, United States. E-mail: akwilbee@hotmail.com*
2 *Graduate Research Asst., Lyles School of Civil Engineering, Purdue University, West Lafayette, United States. E-mail: fpena@purdue.edu, jcondori@purdue.edu*
3 *Graduate Research Asst., School of Mechanical Engineering, Purdue University, West Lafayette, United States. E-mail: zxsun152@gmail.com*
4 *Professor, Schools of Mechanical and Civil Engineering, Purdue University, West Lafayette, United States. E-mail: sdyke@purdue.edu*

ABSTRACT
Dynamic hazards present a challenge to the structural designer. Structural control devices offer one effective approach to protect structures during these dynamic hazards. Various classes of control systems have been explored in recent years and have been demonstrated to be effective for reducing structural responses to extreme events. However, the design of advanced damping systems has not been addressed from the broad perspective of performance. Recent interest in Consequence Based Engineering (CBE) has opened an avenue to change that. CBE works to incorporate the predicted performance of a structure as a factor in its design. This research seeks to demonstrate the potential use of the fragility analysis of controlled structures in CBE. Specifically, this study investigates the sensitivity in the fragility of seismically excited buildings to various passive control configurations. A benchmark model of a 20-story structure is employed. Magneto-rheological (MR) dampers, subject to a constant voltage, act as the source of passive damping for these models. Through these studies, we demonstrate the utility of fragility analysis as a design and modeling tool for eventual use as a facet of CBE.

KEYWORDS: *fragility analysis, passive structural control, dynamic hazard mitigation*

1. INTRODUCTION

Over the last thirty years, the use of structural control has gained attention in the Civil Engineering community. Indeed, the design and implementation of such systems has garnered recognition in the community because of their capability to protect structures against natural hazards and aid in rehabilitation due to aging or deficiency in the design or construction processes (Soong and Spencer, 2002). Control systems are classified as passive, active, or semi-active, according to the energy needed for their operation. Passive systems operate without adding energy to the structure, and are thus inherently stable. Instead, they enhance the energy dissipation capacity of structures by introducing friction, yielding, phase transformation, or deformation of viscoelastic fluids (Soong and Spencer, 2002). This dissipation takes place as a response to the intrinsic movement of the structure. Alternatively, active systems use feedback and have the ability to control specific responses of structures with real-time exchanges between the sensors, controllers, and actuators. This class of devices demands significant additional energy for operation. Without proper attention to the design process, this injection of energy has the potential to lead to instability in the structure. Semi-active systems offer a compromise between passive and active operation. They require a modest amount of supplemental energy, and essentially act as controllable passive devices.

Typically, validation of these control systems is realized by comparing the performance of the uncontrolled and controlled structures for a small suite of representative ground motions. However, these chosen earthquakes only represent a reduced number of data points. This inhibits decision-makers from fully understanding the potential performance that the controlled structure can achieve. For this reason, fragility analysis is an attractive option for informing designers and owners. Fragility analysis assesses a particular aspect of performance, for example, the drift between stories of a building, and expresses the likelihood for which a limit state of that aspect will be exceeded at a certain hazard condition. More formally, it is defined as the conditional probability of a system or component meeting or exceeding a prescribed performance limit state given the occurrence of a particular demand or hazard (Taylor, 2007). This analysis method is less complex and costly than a fully coupled risk analysis, easy to understand, uses a wide range of regionally representative hazards, and can be simply summarized in a single figure, a fragility curve (Taylor, 2007).

Researchers have identified some important findings related to fragility analysis, especially concerning the description of fragility curves. According to an analysis by Wen et al. (2004), it is necessary to quantify the uncertainties present in each structure, such as the variation in material properties and component geometry, since this uncertainty is highly correlated to the slope of the fragility curve. Additionally, the same research exposed the importance of choosing appropriate limit states and representative hazards. These limit values should be chosen with respect to the predominant material of the structure, be clearly tied to structural responses that have a strong relationship with the input hazards, and should agree with the performance level that is desired for the analysis. Furthermore, Jeong and Elnashai (2006) proposed the implementation of a response database of the structure to reduce the computation time for obtaining the fragility curves. This technique, called the Parameterized Fragility Method, consists of evaluating the stiffness, strength and ductility of the structure and comparing the displacement of an equivalent single degree of freedom (SDOF) system and the mode shape with the largest participation. This is done with the purpose of obtaining the mean and standard deviation of the displacement of this equivalent system. These displacement values are then used to calculate the fragility curve in a reduced time by running all the less complex numerical simulations and storing these results in the data base. Subsequently, Taylor (2007) performed a detailed analysis of fragility curves in controlled structures, evaluating fragility curves for different locations and types of control devices in a nonlinear model of a structure. The study demonstrated that the implementation of control devices generated a reduction in the probability of exceedance for different limit states. Also, fragility curves for the passive and active control systems were found to be very similar for small magnitudes of disturbances, measured in this case as spectral acceleration caused by ground motions. However, for large ground motions the passive case had a better performance due to the lack of recognition of the nonlinear behavior of the structure in the design of the active controller. One of the principal findings in Taylor's (2007) research is the better correlation between the responses of the structure and the spectral acceleration, instead of the peak ground acceleration, of the ground motions. Recently, Ryan et. al (2013) computed fragility curves by testing in multiple occasions non-structural elements in a real size structure. This study exposed the differences for multiple configurations of ceilings, wall partitions, and sprinklers in terms of probability of exceedance.

The aforementioned research, as well as other literature in this field, focuses primarily on comparing the performance of structures implementing a few cases of control systems and determining the nature of the analysis itself. However, there has yet to be a focused study on the effects of variation in a control strategy for a representative structure. Here we discuss an analysis of multiple configurations of passive control systems. A comparison of fragility curves of a 20-story linear benchmark structure model is presented under various control force levels. These passive device force levels will be increased incrementally by the modification of the number of nonlinear MR dampers applied to the structure. Two noteworthy trends are found and highlighted in the subsequent discussion. First, past a certain threshold, increasing the number of dampers in the structure results in a change in the behavior of the structure with respect to more lightly damped cases. Though in some cases these changes result in lower drifts, the results are often not altogether favorable when including the largest number of devices. Second, distribution of dampers throughout the structure yields a more effective result than a simple concentration of dampers at the base of the structure. Through these results, this study aims to enhance the way in which different passive damping configurations can be evaluated and understood.

2. MODEL FORMULATION

The fragility relationships resulting from this research are dependent on the models of the benchmark structure and MR damper, and the earthquake records used to produce vibrations in the structure.

2.1. 20 Story Benchmark Model

The 20-story benchmark building, standing at 265 ft in height, was developed for the California region (Spencer et al., 1999). This steel structure has 5 - 20 ft bays in the N-S direction and 6 - 20 ft bays in the W-E direction. The perimeter of these bays forms the lateral resistance system, which is composed of steel moment-resisting frames (MRFs). The column pieces are connected by three-tier construction starting in the second floor; thus, the splices are located on the 2^{nd}, 5^{th}, 8^{th}, 11^{th}, 14^{th}, 17^{th}, and 19^{th} stories. At these floors there is a change in stiffness associated with the location of the splices. One of the two N-S MRFs is modeled directly in the benchmark problem.

Considering a shear model, boundary conditions, modal damping, and static reduction of DOFs the equation of motion, the final state-space representation of the system can be expressed as

$$\mathbf{M\ddot{U}+C\dot{U}+KU= -G\ddot{x}_g+Pf} \tag{2.1}$$

$$\dot{\mathbf{x}} = \mathbf{Ax} + \mathbf{Bf} + \mathbf{E}\ddot{x}_g \tag{2.2}$$

$$\mathbf{y}_m = \mathbf{C}_m\mathbf{x} + \mathbf{D}_m\mathbf{f} + \mathbf{F}_m\ddot{x}_g + \mathbf{v} \tag{2.3}$$

$$\mathbf{y}_e = \mathbf{C}_e\mathbf{x} + \mathbf{D}_e\mathbf{f} + \mathbf{F}_e\ddot{x}_g \tag{2.4}$$

$$\mathbf{y}_c = \mathbf{C}_c\mathbf{x} + \mathbf{D}_c\mathbf{f} + \mathbf{F}_c\ddot{x}_g \tag{2.5}$$

where $\mathbf{x} = [\mathbf{U}^T\ \dot{\mathbf{U}}^T]$ is the state vector and $\mathbf{y}_m, \mathbf{y}_e,$ and $\mathbf{y}_c$ are the output vectors. More complete model details are available on the NEEShub database (https://nees.org/resources/2401). The first 10 natural frequencies of the structural model are 0.29 Hz, 0.83 Hz, 1.43 Hz, 2.01 Hz, 2.64 Hz, 3.08 Hz, 3.30 Hz, 3.53 Hz, 3.99 Hz, and 4.74 Hz. The spectral acceleration of the structure is determined with respect to the first mode natural frequency. Maximum interstory drifts, normalized by the height of floors, are recorded in each earthquake simulation to develop the fragility curves.

For modeling the application of control forces, dampers are concentrated at a central location on each story, attaching to the rigid floor systems both above and below. These rigid floors act to transfer the force of the damper throughout the story.

2.2. MR Damper Model

The passive device used in this study is an MR damper operating in a passive mode with a constant 7.5V. A nine parameter Bouc-Wen model is used to represent the damper to the benchmark structure. This model, presented in Figure 2.1, is widely used for successfully predicting the nonlinear behavior of dampers (Yoshida, 2003):

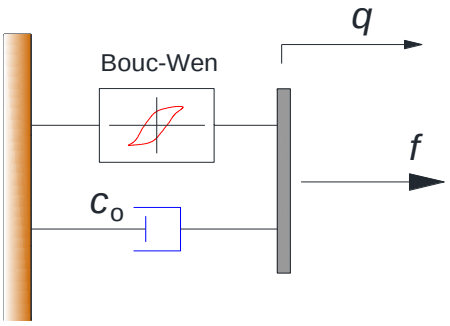

Figure 2.1: Bouc-Wen Damper Model

The force (f) provided by the damper is governed by the following equations, where v is the command voltage to the control circuit, q is the displacement of the device, and z is an evolutionary variable accounting for the history dependence of the response.

$$f = c_0\dot{q} + \alpha z \qquad \dot{z} = -\gamma|\dot{q}|z|z|^n - \beta\dot{q}|z|^n + A\dot{q} \tag{2.6}$$

$$\alpha = \alpha(u) = \alpha_a + \alpha_b u \qquad c_0 = c_0(u) = c_{0a} + c_{0b}u \tag{2.7}$$

$$\dot{u} = -\eta(u - v) \tag{2.8}$$

The remaining variables in these equations are constants that shape the nature of the damper's behavior. To operate with the 20-story structure Yoshida (2007) established a damper model with a 1000kN capacity and a 10V control voltage, scaled from the identified model of a shear-mode prototype MR damper. Thus, here the parameters are chosen as α_a= 1.0872e5 N/cm, α_b= 4.9616e5 N/(cm-V), c_{0a}= 4.40 N-sec/cm, c_{0b}= 44.0 N-sec/(cm-V), A= 1.2, γ= 3 cm^{-1}, β= 3 cm^{-1}, and η= 50 sec^{-1}. For the purposes of this study, the control voltage is taken as a constant of 7.5V, replicating a passive mode of this device. The MR damper model is used in simulation to readily replicate the nonlinear effects of a realistic hysteretic damper on a structure, as well as to prepare for future comparison and implementation of semi-active control cases.

2.3. Sample Earthquakes

The sample earthquakes used in this study are SAC ground motions, which are time histories of generated earthquakes used for case studies and trial applications (Woodward-Clyde, 1997). The particular earthquakes used were generated as being representative of the Los Angeles area, which is where the 20 story benchmark structure was designed to be located (Friedman, 2012; Spencer et. al, 1999). The peak ground accelerations of these earthquakes range from 0.11g – to 1.33g, with spectral accelerations with respect to the first mode of the benchmark structure ranging from 0.19g – 1.86g. A total of 60 SAC earthquakes were used in simulation to express the fragility curves discussed in Section 3.

2.4. Fragility Relation

According to Taylor (2007), the formulation of a fragility curve is dependent primarily on two inputs, the structural response demand (*D*) and the hazard intensity (*S*). In this case, *D* corresponds to the maximum height normalized drift and *S* corresponds to the spectral acceleration of the structure with respect to the input earthquake. They are related according to

$$D = aS^b \tag{2.9}$$

where *a* and *b* are unknown coefficients determined by the logarithmic transformation of Eqn. 2.9. With this information, the fragility can be calculated by

$$F_R = P(D \geq d_0 | S = s) = 1 - \Phi\left(\frac{\lambda_{CL} - \lambda_{D|S}}{\sqrt{{\beta_{D|S}}^2 + {\beta_{CL}}^2 + {\beta_M}^2}}\right) \tag{2.10}$$

where Φ is the standard normal distribution, λ_{CL} = ln(median drift capacity for a particular limit state), $\lambda_{D|S}$ = ln(calculated median demand drift given the spectral acceleration from the best fit power law line), $\beta_{D|S} = \sqrt{ln(1+s^2)}$ [demand uncertainty], $s^2 = \sum\left(ln(Y_i) - ln(Y_p)\right)^2/(n-2)$ [standard error], where Y_i and Y_p are the observed and power law predicted demand drifts, respectively, β_{CL} is the capacity uncertainty, and β_M is the modeling uncertainty. β_{CL} and β_M are taken as 0.3 here, due to the use of those values in similar studies.

Table 2.1 describes the limit states used in this research. The immediate occupancy (IO) state relates to the amount of drift the building may experience while still remaining operational for occupancy immediately post-event. The life safety (LS) state relates to the drift condition that allows the structure to maintain its integrity and be economically repaired, though not necessarily immediately reoccupied.

Table 2.1 Limit State Definition (Cha et. al, 2014)

Maximum Inter-story Drift (%)	Median Demand Drift used with $\lambda_{D\|S}$	Limit State
0.5<Δ< 0.7	0.6	Immediate Occupancy
1.5<Δ< 2.5	2.0	Life Safety

2.5. Cases of study

To consider a range of damping configurations possible in a 20 story structure, some representative cases are identified for analysis. These configurations are chosen based on their potential to represent the most realistic and yet extreme damper distributions for a 20 story structure. For consistency in the naming convention used, all configurations discussed in Section 3 are to be identified with respect to their case number and the number of dampers on floor 1, see Table 2.2.

All cases are simulated using the SAC earthquakes to determine the fragility of the structure with respect to each damping configuration. For each instance, a range of damping strengths will be examined through the use of increasing numbers of model dampers. Cases 5 and 6 will then be evaluated and compared with Cases 1-4, with Cases 1-4 utilizing 60 dampers total in their setups. These evaluation scenarios facilitate a better understanding of the effects of the damping configurations both due to the increase in damping force level within a certain configuration, and with equivalent damping force levels across configurations.

Table 2.2 Description of Cases Selected for Evaluation and Discussion

Case 1	Each floor allocated an equal number of dampers.
Case 2	All dampers concentrated at the first floor.
Case 3	The first ten floors of the structure assigned dampers, with floors 1-5 allocated twice as many dampers as floors 6-10.
Case 4	The first three floors allocated an equal number of dampers.
Case 5	A total of 60 dampers are distributed such that floors 1-7 have 4 dampers, floors 8-15 have 3 dampers, floors 16-18 have 2 dampers, and floors 19 and 20 have 1 damper.
Case 6	A total of 60 dampers are distributed such that floors 1 and 2 have 12 dampers, floors 5 and 8 have 8 dampers, floor 11 and 14 have 6 dampers, and floors 17 and 19 have 4 dampers.

3. RESULTS AND DISCUSSION

In this section we present a number of simulated cases considering the identified damper distributions. Cases 1-4 are first compared against the uncontrolled case by increasing the number of dampers in each configuration. Through this comparison, the benefits of additional dampers are examined. Next, a comparison of different damper layouts is examined. In this comparison, each case considers an equal number of dampers, but with a different distribution throughout the structure. We examine the significance of different damping configurations.

3.1. Discussion of Case 1

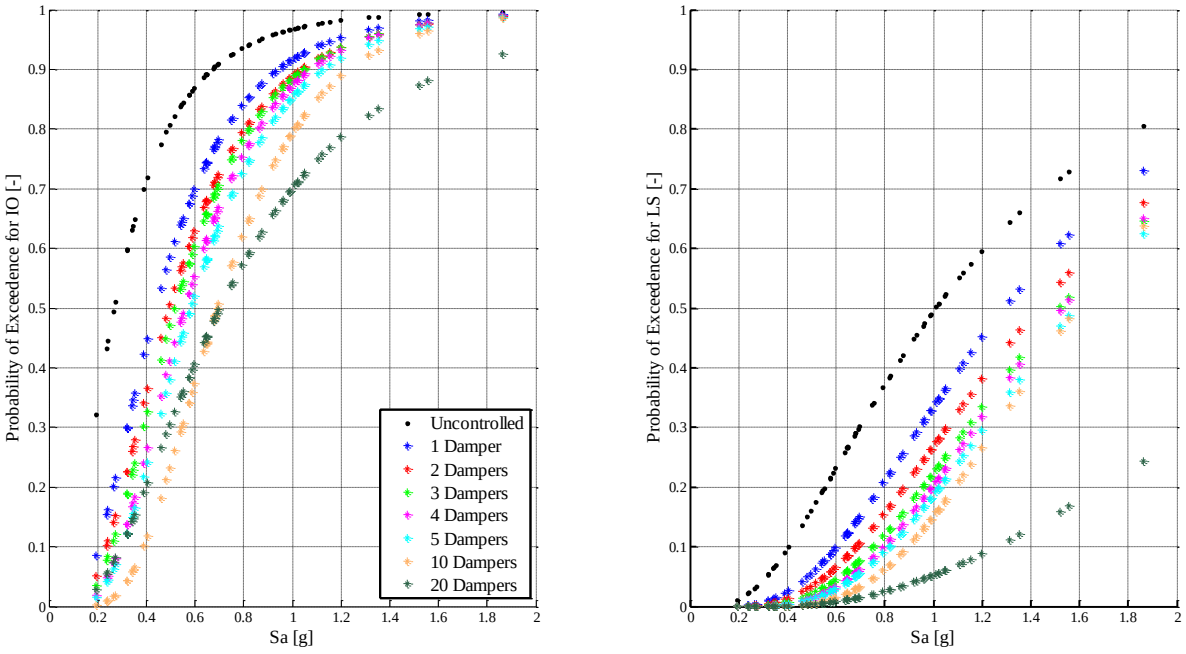

Figure 3.1 Fragility of Different Damping Configuration for the Limit States of IO (Left) and LS (Right)

The fragility curves displayed in Figure 3.1 enable visualization of two significant observations in the results. First, note that a significant reduction in the probability of exceedance is achieved by a single damper on each floor. The maximum reduction achieved by the 1 damper setup is 30% in the IO case and 16% in the LS case. Overall, the maximum reduction is 60% in the IO case (10 Dampers) and 56% in the LS case (20 Dampers). This result demonstrates the efficacy of the supplemental dampers in improving the performance of a structure. The second significant result relates to the behavior of the configuration that includes 20 dampers on each floor, which is admittedly a relatively large number for this particular structure. As seen in both plots, this configuration increases the probability of exceedance with earthquakes having a spectral acceleration of 0-0.7 g. However, for spectral accelerations above that range, this configuration represents a 56% reduction, as illustrated by the maximum reduction in the LS limit state. This result is particularly important as it represents a deviation from the trends experienced by the 1-10 damper setups. For setups with 1-10 devices per floor, the effectiveness of increasing the number of dampers diminished with each damper added. However, the behavior of the configuration with 20 damper per floor breaks this pattern, instead suggesting that the addition of

excessive damping to the structure, at least in an evenly distributed damping case, has the potential to change the nature of fragility curve. The configuration with 20 dampers per floor becomes highly efficient at reducing the largest drifts in the structure at high amplitude vibrations, but begins to lose its ability to regulate low amplitude vibrations.

3.2. Discussion of Cases 2-4

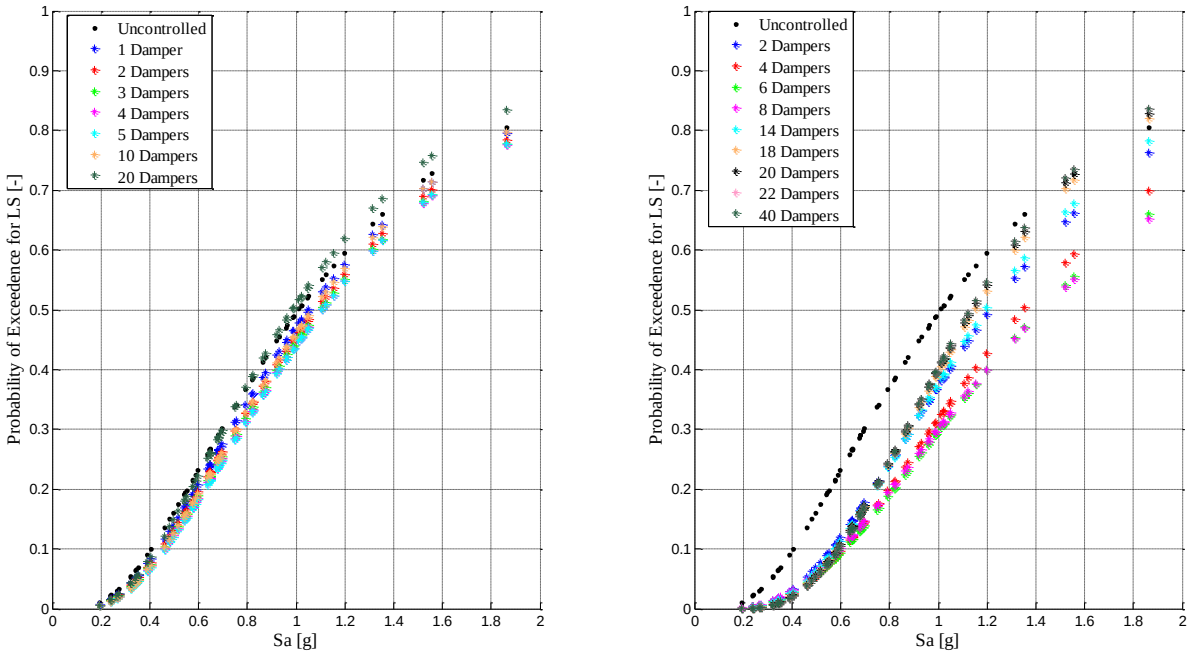

Figure 3.2 Fragility of Case 2 (Left) and Case 3 (Right) with Respect to the LS Limit State

The results shown in Figure 3.2 (left) for Case 2 represent the other extreme of the damper placement spectrum, with all dampers located at the first floor of the structure. This configuration produces less improvement in performance than does Case 1, with a maximum reduction from the uncontrolled case of 5% in the IO case (2 dampers) and 6% in the LS case (5 dampers). Note the reversal that occurs here in both the 10 and 20 damper setups, which is similar to the reversal occurring in Case 1. However, with this particular layout, there is a threshold at which the addition of dampers to the first floor actually increases the probability of exceedance to a level greater than that of the uncontrolled case. This result suggests, as it did in Figure 3.1, that the over-damping creates a lock-up behavior in the structure. Due to excessive damping on the first floor, the first story appears to act more rigidly, transferring more vibrations from the ground to the upper floors of the structure and resulting in larger floor drifts overall. This behavior is aided by the fact that, in contrast with Case 1, placing dampers on only the first floor allows damping at none of the floors with splices. A lack of control in the spliced floors creates the potential for the structure to experience greater drift in those floors as the first floor becomes increasingly rigid.

Though the maximum reductions in the probability of exceedance are slightly different, with a maximum reduction of 11% in the IO case (3 dampers) and 9% in the LS case (4 dampers), the results from Case 4 tell the same story as the Case 2. The reversal in the effectiveness of additional damper placement still occurs with 10 dampers per floor and results in the uncontrolled case being exceeded by 5% in the configuration with 20 dampers per floor. The increased performance in this damping case seems to align with the control of more floors, and one splice, in the structure.

The second graph in Figure 3.2 (right) shows the effects of dampers added to the Case 3 damping configuration. This case seems to transition between the effects of Case 1 and Case 2. Here the damping is focused on the lower half of the building, and provides damping force at half of the floors with splices. Case 3 experiences the same reversal as the other cases, although it occurs after a maximum reduction in the probability of exceedance of 20% in the LS case through the use of the 8 damper setup. The maximum reduction for the IO setup is 25% (40 dampers). Note that the variation in performance reversals between cases 1-4 demonstrates the utility of a fragility curve for examination of the performance of damping and control systems over a broad range of

seismic amplitudes. These particular trends would be difficult to fully comprehend through the independent examination of a few response histories. Through the holistic view of a fragility curve, these trends are more easily visualized and analyzed.

3.3. Discussion of the Various 60 Damper Distributions

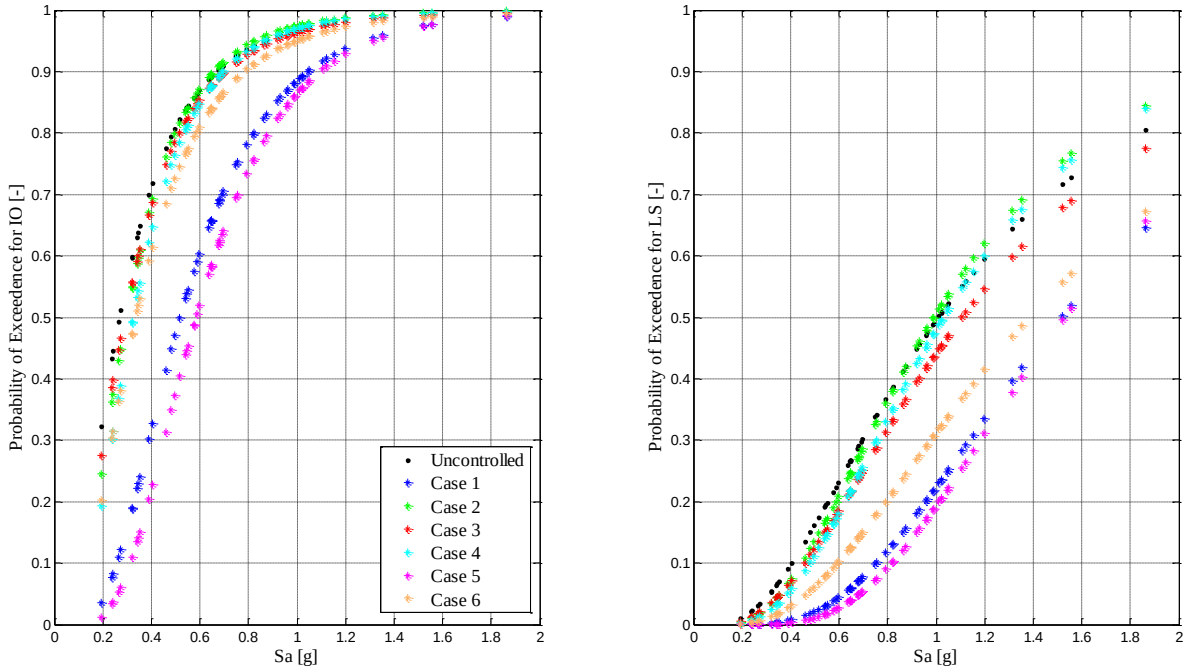

Figure 3.3 Fragility of 60 Damper Configurations with Respect to the Limit States of IO (Left) and LS (Right)

In an effort to compare the effect of different damper configurations while keeping the cost, i.e. the number of dampers, the same, Cases 1-6 were simulated with configurations that employ a total of 60 dampers. For the most part, the limit states displayed in Figure 3.3 convey the same information. When each configuration has an equal numbers of dampers, the configuration of those dampers within the structure strongly affects its fragility. The maximum reduction in the probability of exceedance between Case 1 and Case 2 is 37% in the IO case and 28% in the LS case. This reduction is notably large, even though the same number of dampers is used. This result indicates that the concentration of damping at the base of the structure is clearly not the most effective strategy, which supports and agrees with the general approach used for control design. It instead suggests that organizing the available damping power throughout the structure in an optimized manner, as is shown in Case 5, will produce the greatest gains in performance. Overall, this case produces a maximum reduction of 50% in the IO case and 30% in the LS case. Concentrating the damping toward the bottom floors of the structure, while still continuing to add damping throughout the structure, appears to create the largest reductions for the 20 story benchmark building while also having the least cost associated with damping power. For example, to approximate this result using the configuration in Case 1, a 5 damper setup would be required. That configuration would use 100 dampers, much more than that used in Case 5. This result seems to be generally true for the benchmark structure, likely due to the splices spaced every three floors throughout the structure. An optimized damping scheme thus allows for concentrating the damping closer to the ground where the vibrations impact the building, while still controlling the drift around the weak points in the upper floors.

Case 6 further demonstrates the potential of adding dampers in key locations in the structure. In this case, the damping is concentrated at the first floor but also at the floors containing splices where significant changes in stiffness occur. Though it does not approach the success of Cases 1 and 5, this case indicates the significance of damping around splices, as this approach reduces the probability of exceedance of the structure beyond Cases 2-4 by 13% in the IO limit state and 18% in the LS limit state. It is interesting to note that the relative effect of this strategy is different for each limit state. In the IO case, the damping strategy produces effects similar to Cases 2-4. However, in the LS state this strategy produces fragility curves that lie between Cases 2-4 and Cases 1 and 5, eventually drifting closer to Case 1. This outcome indicates that the strategy is more effective at reducing the displacements to a normalized drift below 2% than it is at reducing the drift below 0.6%. This observation is explained by the fact that several floors in the structure remain uncontrolled (no dampers). The

strategy thus reduces the drift to such a point that Case 6 performs well in the LS range, while allowing the structure to produce relatively larger drifts at the uncontrolled floors, resulting in the curves in Figure 3.3.

4. CONCLUSIONS

Through the use of fragility curves as a visualization and performance evaluation tool, this research has demonstrated two major observations in the passive control of the 20 story linear benchmark structure. First, the fragility curves show that increasing the number of dampers beyond a certain threshold can change the behavior of the structure with respect to more lightly damped cases. The fragility curves may cross over each other at a certain spectral acceleration level. This observation has been reported by other researchers in isolated cases (Dyke et al., 1998), but the use of fragility curves facilitates visual evidence of this behavior. Second, intelligent distribution of damping effort throughout the structure results in a more effective technique for improving performance than a concentration of dampers at the base of the structure. This result is particularly true if the dampers are placed to provide added damping in key locations, such as at floors that contain splices, as demonstrated through this benchmark case. These results demonstrated that fragility curves provide an alternative approach in which one may examine the effectiveness of different passive damping configurations.

In future studies we will expand this work to examine and compare the fragility of a more comprehensive set of passively, actively and semi-actively controlled structures using both linear and nonlinear building models.

ACKNOWLEDGEMENT

This research is partially supported by National Science Foundation Grant No. 1148255. The second and third authors, respectively, acknowledge the support of the Department of Science, Technology, and Innovation - COLCIENCIAS and the Colombia-Purdue Institute for Advanced Scientific Research, as well a the National Council for Science, Technology and Technological Innovation - CONCYTEC, Peru. This support is gratefully acknowledged.

REFERENCES

1. Cha, Y.-J., Agrawal, A.K., Phillips, B.M., Spencer Jr., B.F. (2014). Direct performance-based design with 200 kN MR dampers using multi-objective cost effective optimization for steel MRFs. *Engineering Structures*. **17**, 60-72.
2. Friedman A. J. (2012). Development and Experimental Validation of a New Control Strategy Considering Device Dynamics for Large-Scale MR Dampers using Real-Time Hybrid Simulation. *PhD Dissertation, Purdue University, Department of Civil Engineering.* West Lafayette, Indiana.
3. Jeong, S.-H., and Elnashai, A.S. (2006). New three-dimensional damage index for RC buildings with planar irregularities. *Journal of Structural Engineering* **132: 9**, 1482-1490.
4. Yoshida, O. (2003). Torsionally Coupled Response Control of Earthquake Excited Asymmetric Buildings: Development and Application of Effective Control Systems Using Smart Dampers. *PhD Dissertation, Washington University in St. Louis, Sever Institute of Technology, Department of Civil Engineering.* Saint Louis, Missouri.
5. Spencer, B.F., Jr., Christenson, R.E. and Dyke, S.J. (1999). Next Generation Benchmark Control Problem for Seismically Excited Buildings. *Proc., 2nd World Conf. on Structural Control*, (T. Kobori, et al., eds., Wiley), **2**, 1135-1360.
6. Soong, T.T., and Spencer Jr., B.F. (2002). Supplemental energy dissipation: state-of-the-art and state-of-the-practice. *Engineering Structures*. **24: 3**, 243-259.
7. Soroushian, S., Ryan, K. L., Maragakis, M., Wieser, J., Sasaki, T., Sato, E., Okazaki, T., Tedesco, L., Zaghi, A.E., Mosqueda, G., Alvarez, D. (2012). NEES/E-Defense tests: Seismic performance of ceiling/sprinkler piping nonstructural systems in base isolated and fixed base building. *15th World Conference on Earthquake Engineering (15WCEE)*. Lisboa, Portugal.
8. Taylor, E. D. (2007). The development of fragility relationships for controlled structures. *M.S. Thesis., Washington University, Department of Civil Engineering.* Saint Louis, Missouri.
9. Wen, Y. K., Ellingwood, B., and Bracci, J. M. (2004). Vulnerability function framework for consequence-based engineering. *MAE Center Report.* **4: 4**.
10. Woodward-Clyde Federal Services. (1997). Develop Suites of Time Histories: SAC Joint Venture Steel Project Phase 2. http://nisee.berkeley.edu/data/strong_motion/sacsteel/draftreport.html
11. Dyke, S.J., Spencer Jr., B.F., Sain, M.K. and Carlson, J.D. (1998). "An Experimental Study of MR Dampers for Seismic Protection," *Smart Matl. & Struc.: Spec. Issue on Large Civil Struc.*, **7**, 693-703.